INT. J. REMOTE SENSING, 2001, VOL. 22, NO. 7, 1285–1303

Validation of coastal sea and lake surface temperature measurements derived from NOAA/AVHRR data

X. LI†, W. PICHEL‡, P. CLEMENTE-COLÓN‡,
V. KRASNOPOLSKY§ and J. SAPPER‡

†Research and Data Systems Corporation, Room 102, E/RA3, WWBG, NOAA Science Center, 5200 Auth Road, Camp Springs, Maryland 20746-4304, USA; e-mail: xiaofeng.li@noaa.gov
‡NOAA/NESDIS, Room 102, E/RA3, WWBG, 5200 Auth Road, Camp Springs, Maryland 20746-4304, USA
§General Sciences Corporation, 6100 Chevy Chase Drive, Laurel, Maryland 20707, USA

(*Received 11 January 1999; in final form 20 December 1999*)

Abstract. An interactive validation monitoring system is being used at the NOAA/NESDIS to validate the sea surface temperature (SST) derived from the NOAA-12 and NOAA-14 polar orbiting satellite AVHRR sensors for the NOAA CoastWatch program. In 1997, we validated the SST in coastal regions of the Gulf of Mexico, Southeast US and Northeast US and the lake surface temperatures in the Great Lakes every other month. The *in situ* temperatures measured by 24 NOAA moored buoys were used as ground data. The non-linear SST (NLSST) algorithm was used for all AVHRR SST estimations except during the day in the Great Lakes where the linear multichannel SST (MCSST) algorithm was used. The buoy–satellite matchups were made within one image pixel in space (1.1 km at nadir) and ± 1 h in time.

For the NOAA-12 satellite, the validation results for the three coastal regions (Gulf of Mexico, Southeast US and Northeast US) showed that the mean temperature difference between satellite and buoy surface temperature (bias) was about 0.4°C during the day and 0.2°C at night. The standard deviation was about 1.0°C. Great Lakes validation results showed a bias less than 0.3°C during the day. However, due to the early morning fog situation in the summer months in the Great Lakes region, the NLSST night algorithm yielded a fairly large bias of about 1.5°C.

The same statistics were computed for the NOAA-14 satellite measurements. For the coastal regions, the bias was less than 0.2°C with a standard deviation about 1.0°C. For the Great Lakes region, the bias was about 0.4°C for both day and night with a standard deviation about 1.0°C.

Our study also showed that the NLSST algorithm provides the same order of SST accuracy over all study regions and under a wide range of environmental conditions.

1. Introduction

The derivation of sea surface temperature (SST) from satellite measurements has been a focus of numerous studies since the early 1970s (Anding and Kauth 1970, McMillin 1975, McMillin *et al.* 1975, Barton 1983, Llewellyn-Jones *et al.* 1984,

ISSN 0143-1161 print/ISSN 1366-5901 online
http://www.tandf.co.uk/journals

McMillin and Crosby 1984, McClain *et al.* 1985, Walton 1988, Barton *et al.* 1989, Minnett 1990, Emery *et al.* 1994, Walton *et al.* 1998). The Advanced Very High Resolution Radiometer (AVHRR/2) onboard the NOAA series of Polar-orbiting Operational Environmental Satellites (POES) is primarily designed for SST retrieval and cloud detection. POES satellites known as Advanced Television Infrared Observation Satellites (TIROS-N or ATN) operate as a pair to ensure that the data, for any region of the earth, are no more than 6 h old. AVHRR has five channels, two visible channels (channels 1 and 2 at 0.6 and 0.9 μm, respectively), one short-wavelength infrared channel (channel 3 at 3.7 μm), and two long-wavelength infrared channels, the split window channels (channels 4 and 5 at 11 and 12 μm, respectively). The wavelengths of the three infrared channels are selected in a range of the electromagnetic spectrum in which the radiation from the earth's surface and clouds is only weakly attenuated. To determine the actual SST from the AVHRR radiation measurements, one must correct for absorption and reemission of radiation by atmospheric gases, predominately water vapour. The split window method, which uses the channel 4 and 5 brightness temperatures to calculate SST, is widely used for atmospheric correction. A summary and comparison of different split window algorithms are given in Barton (1995).

NOAA's National Environmental Satellite, Data, and Information Service (NESDIS) produces two main types of SST products; i.e. global SST and CoastWatch SST. The global SST suite of products are generated from AVHRR Global Area Coverage (GAC) 4 km data recorded on-board the POES satellites and downlinked to NESDIS acquisition stations at Wallops Station, Virginia and Fairbanks, Alaska. Global SST measurements are produced at 8 km resolution with variable spacing from 8 to 25 km in cloud-free areas twice per day from each of the two operational POES satellites. The global satellite SST measurements are validated by comparing them with drifting buoy (and TOGA moored buoys in the tropical Pacific) SST measurements matching within 4 h and 25 km. These global satellite SST measurements are used to produce SST analyses at grid resolutions from 14 to 100 km. CoastWatch SST products are generated from a different data stream, the AVHRR High Resolution Picture Transmission (HRPT) data, broadcast continuously by the POES satellites. The HRPT data have a resolution of 1.1 km at nadir and are mapped to almost full resolution in the production of CoastWatch AVHRR visible, infrared and SST images. The CoastWatch products are validated by comparison with NOAA moored buoy SST reports using techniques described herein. Figure 1 shows the time lines of different operational algorithms used at NOAA/NESDIS. Based on the split window theory, the multichannel SST (MCSST) algorithm was developed and used operationally at NOAA/NESDIS in the early 1980s. This algorithm assumes that there is a linear relationship between the difference of the actual SST and a satellite measurement in one channel and the difference of satellite measurements in the split window channels (channel 4 and 5). Therefore, the actual SST can be estimated using brightness temperatures measured with channels 4 and 5. Walton (1988) considered a non-linear term in the further development of MCSST and developed the cross-product SST (CPSST) algorithm. A simple version of the CPSST algorithm, called the non-linear SST (NLSST) algorithm, was implemented at NESDIS for operational use in April 1991. The coefficients for these algorithms are routinely obtained by performing a regression between satellite retrievals and buoy data soon after each satellite's launch.

Satellite-derived SST imagery has been widely used in studying atmospheric and

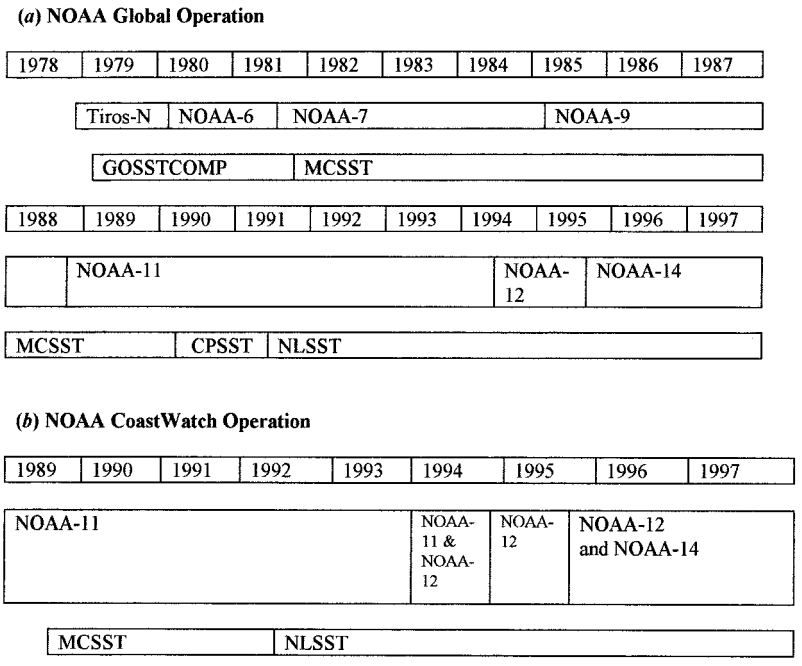

Figure 1. Time lines of NOAA series of polar orbiting satellites used for SST and the operational sea surface temperature algorithms used at NOAA/NESDIS. (*a*) NOAA Global Operation, (*b*) NOAA CoastWatch Operation. GOSSTCOMP: Global Operational Sea Surface Temperature Computation. MCSST: Multichannel Sea Surface Temperature, the MCSST product started on 17 November 1981. CPSST: Cross-product sea surface temperature, beginning 2 March 1990. NLSST: Non-linear Sea Surface Temperature, NLSST product, starting on 10 April 1991 in the global operation and on 3 June 1992 in the CoastWatch operation.

oceanic problems. For some applications, relatively low absolute SST accuracy is required as long as high relative accuracy is achieved, i.e. for front and edge detection (Cayula and Cornillon 1992, Kahru *et al.* 1995), and in feature tracking and motion detection (Emery and Fowler 1991, Breaker *et al.* 1994). However, in some other studies, i.e. climate studies (Harries *et al.* 1983, Yates *et al.* 1985, Cornillon 1989), a more stringent absolute SST accuracy, normally less than 0.3°C, is required. To understand the satellite-derived SST accuracy, scientists have performed various validation efforts by comparing the AVHRR measurements with moored buoy, drifting buoy and ship measurements in the global ocean as well as in different coastal regions.

For the global GAC SST validation, Strong and McClain (1984) used the data between November 1981 and February 1982 and found that the root mean square (rms.) error of the temperature difference between satellite and *in situ* measurement was between 0.6 and 1.8°C. Pichel (1991) used 3 months of a NOAA-11 satellite and buoy matchup dataset between March and May 1990 to validate the NLSST algorithm, and found the accuracy had been improved. The global mean satellite–buoy difference (or bias) was less than 0.3°C with a standard deviation of about 0.7°C. Walton *et al.* (1998) analysed a 9-year time series of satellite–buoy matchups between 1989 and 1997. They showed that the bias has stayed between -0.2 and 0.4°C over the 9-year period, while the scatter of the difference between the satellite and buoy

SSTs improved from 0.8 to 0.5°C for the daytime algorithm but remained about 0.5°C for the night-time algorithm. In their study, satellite–buoy matches were constrained to 25 km and 4 h. The largest differences resulted from the volcanic aerosols from the Mt Pinatubo eruptions in October 1992, with a positive bias in the night-time SST measurements observed from the month of the eruptions until June 1993.

The matchups made within 4 h in the global SST validation can be less accurate when a diurnal warming effect is considered (Cornillion and Stramma 1985, Böhm *et al.* 1991, Hawkins *et al.* 1993). For regional validations, one needs to set up satellite–buoy matchup datasets at higher spatial and temporal resolutions than are used in global validation studies. So far, there have been only a few studies concerning regional AVHRR SST validation. Pearce *et al.* (1989) validated the NOAA-7 and NOAA-9 satellite-derived SST using *in situ* boat measurements as ground data in the coastal waters off Western Australia. They compared seven published split window algorithm derived SSTs and found that all algorithms yielded reasonably good results. The rms. error between SSTs calculated with two of the algorithms and their corresponding ship measurements was about 0.6°C. The bias was between − 0.1 and 0.2°C. Robinson and Ward (1989) compared NOAA-7 SSTs calculated with the Llewellyn-Jones *et al.* (1984) split window algorithm with cruise data in the north-east Atlantic Ocean. The ship and satellite measurement agreement was within 1°C. Yokoyama and Tanba (1991) compared 14 published split window algorithms using a matchup dataset in Mutsu Bay in northern Japan for the NOAA-9 satellite. They showed that the regional split window algorithm had rms. errors in the range of 0.55–0.75°C. In their more recent paper, Yokoyama *et al.* (1993) found that larger satellite retrieval errors appeared to occur when the air–sea temperature difference was large. May and Holyer (1993) noticed the satellite SST retrieval error can be as large as 1°C when the air sea temperature difference changes 10–12°C from the mean conditions in their global dataset. Topliss (1995) reviewed split window algorithms for the NOAA-7, NOAA-9 and NOAA-11 satellites and developed new regional split window algorithms for the Canadian coastal region. All the above regional SST algorithms are linear SST algorithms.

NOAA/NESDIS uses NLSST rather than regional algorithms for the measurement of SST. This avoids the problems of possible discontinuities at the regional boundaries as well as any need for seasonal adjustments within regions (Walton *et al.* 1998). In this study, we use a long-term validation system developed for the NOAA CoastWatch program to validate the accuracy of AVHRR SSTs in the Northeast, Southeast, and Gulf of Mexico coastal regions and lake surface temperatures in the Great Lakes area for NOAA-12 and NOAA-14 in 1997. In §2, CoastWatch AVHRR data preparation is presented, followed by a description of the validation procedure in §3. In §4, we present validation results. Analysis and discussion are in §5, and the conclusions are in §6.

2. NOAA CoastWatch AVHRR data preparation

2.1. *Satellite mapped data for CoastWatch*

CoastWatch is a NOAA program managed by NESDIS with CoastWatch Nodes located at NOAA laboratories and offices in eight coastal states. The goal of CoastWatch is to provide satellite and other environmental data and products for near real-time monitoring of US coastal waters in support of environmental science, management and hazard response. The CoastWatch Nodes generate products or

receive them from NESDIS and make them available to a diverse and growing user community of Federal and state environmental resource managers, research scientists, educators, fishermen, and marine enthusiasts. Products include polar and geostationary satellite infrared, visible, and SST images, as well as ocean colour and Synthetic Aperture Radar (SAR) imagery. Started in 1990, with all eight Nodes operating by 1993, CoastWatch had over 2100 registered users in 1997.

Input data for the production of CoastWatch imagery are HRPT 1b datasets. These consist of AVHRR detector output from the five channels of the AVHRR with appended calibration and earth location information. For US east coast, Great Lakes and Gulf of Mexico regions, datasets are received from every satellite pass over the Wallops Station, Virginia reception mask.

During 1997, the two operational polar orbiting satellites were NOAA-12 and NOAA-14. NOAA-12 was launched on 14 May 1991, into a sun-synchronous polar orbit with equator crossing times early in the morning at 07:09 am descending and in the evening at 19:09 pm ascending. NOAA-14 was launched on 30 December 1994, into a similar orbit with equator crossing times ascending in the afternoon at 13:43 pm local time and descending at night at 01:43 am. Usually, each CoastWatch region receives satellite coverage four times per day. The local satellite overpass times for NOAA-12 and NOAA-14 are given in table 1. Satellite data from Wallops are transmitted to the NESDIS Central Environmental Satellite Computer System (CEMSCS) in Suitland, Maryland as soon as each satellite overpass is completed. Processing into 1b data proceeds automatically as soon as the complete pass has arrived, followed by CoastWatch mapping over each region covered by the satellite pass.

2.2. *CoastWatch mapping*

The AVHRR NOAA level 1b data are mapped to Mercator projection 'region' maps covering entire CoastWatch regions. All five channels, as well as the satellite and solar zenith angles, are mapped at 1.1 km resolution at nadir. The zenith angle is the angle at a point on the earth between the local normal at that point and a line connecting the point on the earth and the satellite or the sun. The satellite zenith angle is computed using the relation:

$$\sin(\theta) = (1 + H/R) \times \sin(\alpha) \tag{1}$$

where θ is the satellite zenith angle, H is the height of the satellite, R is the radius of the earth and α is the scan angle. The scan angle, which is also called the nadir angle, is defined as the angle between the line connecting the satellite with the subsatellite point and a line connecting the satellite to a viewed spot on the earth

Table 1. NOAA-12 and NOAA-14 local (US east coast) overpass times.

Satellite	Time	GMT	Local time (EST)
NOAA-12	Day	21–23Z	4:00–6:00 pm
	Night	11–12Z	6:00–7:00 am
NOAA-14	Day	18–19Z	1:00–2:00 pm
	Night	06–07Z	1:00–2:00 am

scan. For AVHRR scans, the scan angle ranges from 0° to 55.4°. The scan angle, α, is computed using the relation:

$$\alpha = (55.4/N) \times |M - N| \quad (2)$$

where M is any given spot number and N is the spot number of nadir.

For NOAA POES satellites, the range of satellite zenith angles can be shown using equation (1) to be from 0° to 68.4°. The factor H/R in equation (1) is hardcoded in the image processing programs as 0.13, since the NOAA satellite height is about 825 km. If there is a significant variation in satellite height, the satellite zenith angles generated are expected to be off at high zenith angles by 1% for every 50 km difference in altitude. At larger satellite zenith angles, the larger atmospheric path length leads to greater attenuation of surface infrared emissions and thus the need for greater correction of AVHRR channel temperatures when calculating SST. Also, since the field of view increases with satellite zenith angle, there is a greater chance of cloud contamination as zenith angle increases. These effects should lead to a decrease in accuracy of SST measurement at high satellite zenith angles. To maintain high accuracy, no SST measurements are attempted at satellite zenith angles above 53°. The exception to this rule is in the Gulf of Mexico CoastWatch region where spatial coverage was determined to be more important than absolute accuracy.

Each satellite pixel is calibrated to albedo or equivalent blackbody temperature (correcting for non-linearity in the calibration of channel 4 and 5, see Planet 1998) and transformed to a map pixel. Any map pixels left unfilled after all satellite data have been mapped are filled with an average of all the pixels in a 5×5 array about the unfilled pixel. To retain the full radiometric precision of the AVHRR instrument, 11 bits are used to store the calibrated satellite values (Pichel *et al.* 1991).

2.3. *Operational nonlinear SST (NLSST) and multichannel SST (MCSST) algorithms*

Once the data have been mapped, then the multiple channels and angles are combined with multichannel algorithms to produce SST and cloud mask imagery. SST imagery is generated with the non-linear NLSST split window algorithm in the US coastal regions. This algorithm utilizes the difference between the 11 and 12 μm infrared channels to correct for the effects of water vapour. Since infrared radiation is absorbed by atmospheric moisture more within the 12 μm channel than within the 11 μm channel, the temperature difference between these channels is proportional to the amount of water vapour in the atmosphere. The equations also contain a correction for atmospheric path length variation with satellite zenith angle. The linear MCSST split window equation is used to obtain an estimate of the surface temperature for the non-linear term of the NLSST equation. Separate equations are used for day and night data and the equations are satellite dependent. These equations are generated after satellite launch by matching a month's worth of satellite data with global drifting buoy observations. All matches within 25 km and 4 h are used in a regression analysis in order to derive the equations. Because of the global nature of the matchup dataset, the regression equations are usually independent of season, geographic location, or atmospheric moisture content. However, adjustments to the equations have been necessary when instrument or spacecraft environmental changes have effected the calibration, and when volcanic stratospheric aerosols cover large

regions of the Earth. The NLSST and MCSST equations used in CoastWatch are given below:

$$\text{NLSST} = A_1(T_{11}) + A_2(T_{11} - T_{12})(\text{MCSST}) + A_3(T_{11} - T_{12})(\sec\theta - 1) - A_4 \quad (3)$$

$$\text{MCSST} = B_1(T_{11}) + B_2(T_{11} - T_{12}) + B_3(T_{11} - T_{12})(\sec\theta - 1) - B_4 \quad (4)$$

where T_{11} and T_{12} are the AVHRR 11 and 12 μm channel temperatures in Kelvin; $\sec\theta$ is the secant of the satellite zenith angle θ; NLSST and MCSST are the non-linear and linear multichannel SST retrieval algorithms, respectively, in Centigrade; $A_1 - A_4$ and $B_1 - B_4$ are constant coefficients. $A_1 - A_4$ and $B_1 - B_4$ coefficients for the NOAA-12 and NOAA-14 day and night algorithms are given in table 2.

Recently, Walton *et al.* (1998) showed a 9-year time series of NOAA-14 satellite–buoy monthly bias (i.e. mean satellite–buoy SST difference) and scatter (i.e. standard deviation of satellite–buoy SST difference) between 1989 and 1998. Their results show that the improvement in the scatter from 0.8 to 0.5°C is partly due to improved SST algorithms (from MCSST to NLSST), and partly to the improvements in the cloud detection algorithms. Shenoi (1999) accessed the MCSST and NLSST algorithms performance for NOAA-9 and NOAA-11 satellites. Their results showed that the mean and RMSD values of SST residuals estimated by NLSST are better than those estimated by MCSST for both satellites.

The CoastWatch equations differ from the global SST equations in three respects:

1. The CoastWatch equations use the MCSST value in the non-linear term rather than an *a priori* SST estimate obtained from an analysis of past satellite SST data. This means that there is somewhat more noise in the CoastWatch observations. Both the global operation and CoastWatch constrain the value of the *a priori* SST or the MCSST to the range 0–28°C.

2. In the Great Lakes, the MCSST value is used as the final SST value during the day; i.e. a linear equation is used as the operational equation rather than a non-linear equation. In earlier accuracy studies, it was found that the MCSST equations consistently gave slightly more accurate SST measurements than did the NLSST algorithm during the day.

3. The NLSST split-window equation is used for CoastWatch at night rather than the triple-window equation (employing all three infrared channels) which is used in the global operation. For NOAA-12, the 3.7 μm channel is not used for

Table 2. NOAA-14 and NOAA-12 NLSST and MCSST algorithm coefficients used in CoastWatch SST measurements.

NLSST coefficients					
		A_1	A_2	A_3	A_4
NOAA-14	day	0.939813	0.076066	0.801458	255.165
NOAA-14	night	0.933109	0.078095	0.738128	253.428
NOAA-12	day	0.876992	0.083132	0.349877	236.667
NOAA-12	night	0.888706	0.081646	0.576136	240.229
MCSST coefficients					
		B_1	B_2	B_3	B_4
NOAA-14	day	1.017342	2.139588	0.779706	278.430
NOAA-14	night	1.029088	2.275385	0.752567	282.240
NOAA-12	day	0.963563	2.579211	0.242598	263.006
NOAA-12	night	0.967077	2.384376	0.480788	263.940

CoastWatch because there is a problem in the calibration of that channel during part of each orbit. For consistency, the NLSST split-window equation is also used for the NOAA-14 CoastWatch equations.

2.4. *CoastWatch image products*

Once SSTs are generated by the NLSST and MCSST algorithms and maps are generated for each CoastWatch region, the CoastWatch mapping system generates a series of 'sector' images from the region maps. These sector maps are all 512×512 pixels in size for selected areas within the region. Sectors are produced at full-resolution for the validation areas shown in figure 2. Sector maps can be infrared or visible channels, angles, SST or cloud masks. All the sector products as well as the full-resolution region maps are now being archived. In this study, we use the full resolution images to validate the AVHRR SST product.

A cloud-mask image product useful for interpretation of the SST imagery or for automatic multiday composing of cloud-free pixels is also generated. The algorithm employed is the CLouds from AVHRR (CLAVR) algorithm (Stowe *et al.* 1991). With a series of threshold, uniformity, and channel-difference or ratio tests, the CLAVR algorithm determines whether each 2×2 pixel array in the region map is clear or cloudy. The cloud maps are generated in the same projection as the SST images and used as aids in determining the clear satellite–buoy matches used in the validation procedure.

3. NOAA CoastWatch validation procedure

The CoastWatch validation system is an interactive, menu-driven, image and data processing system. The system was developed using the Interactive Data Language (IDL) computer language and can be run on both VAX and UNIX

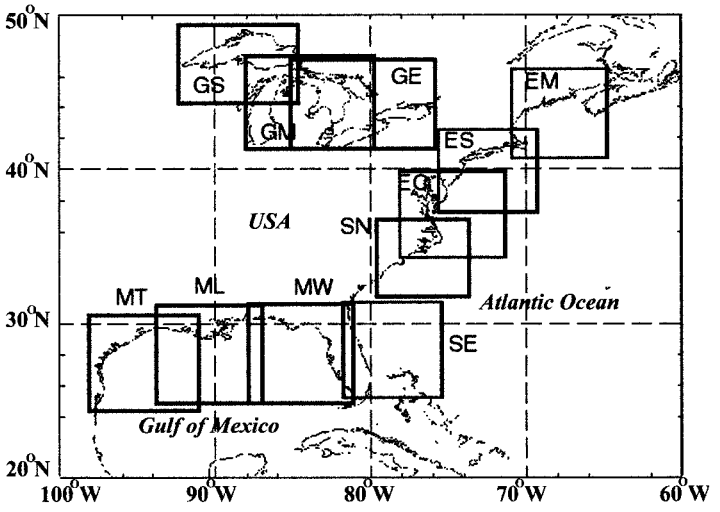

Figure 2. CoastWatch high resolution AVHRR data remapped areas used in the CoastWatch validation system. Great Lakes: Lake Huron, Erie and Ontario (GE); Lake Michigan and Huron (GM); Lake Superior (GS). Northeast: Chesapeake Bay (EC); Gulf of Maine (EM); Southern New England (ES). Southeast: East Florida (SE); North Carolina (SN). Gulf of Mexico: Louisiana and Mississippi (ML); Texas (MT); West Florida (MW).

platforms. This system is designed to provide long-term validation for the CoastWatch SST, visible and cloud-mask imagery. The hierarchy chart of the current validation system is presented in figure 3.

The National Centers for Environmental Predication (NCEP) provides the buoy data used in the matching procedure. These data are placed in the buoy data file four times a day. The buoy data file also gives the current NOAA moored buoy locations, so an analyst can overlay the buoy positions on the AVHRR imagery. AVHRR imagery is in the CoastWatch format and images are archived at the National Oceanographic Data Center (NODC). The main input for this long-term validation system is the Target Match File (TMF). The TMF is generated by extracting 15×15 pixel array targets of the CoastWatch imagery (i.e. mapped full-resolution AVHRR HRPT imagery including all five channels, cloud masks and SST) centred at NOAA moored buoy positions on the NOAA/NESDIS Central EnvironMental Satellite Computer System (CEMSCS) mainframe computer. The corresponding buoy data are appended to each target.

The long-term validation system enables an analyst to (1) preview AVHRR

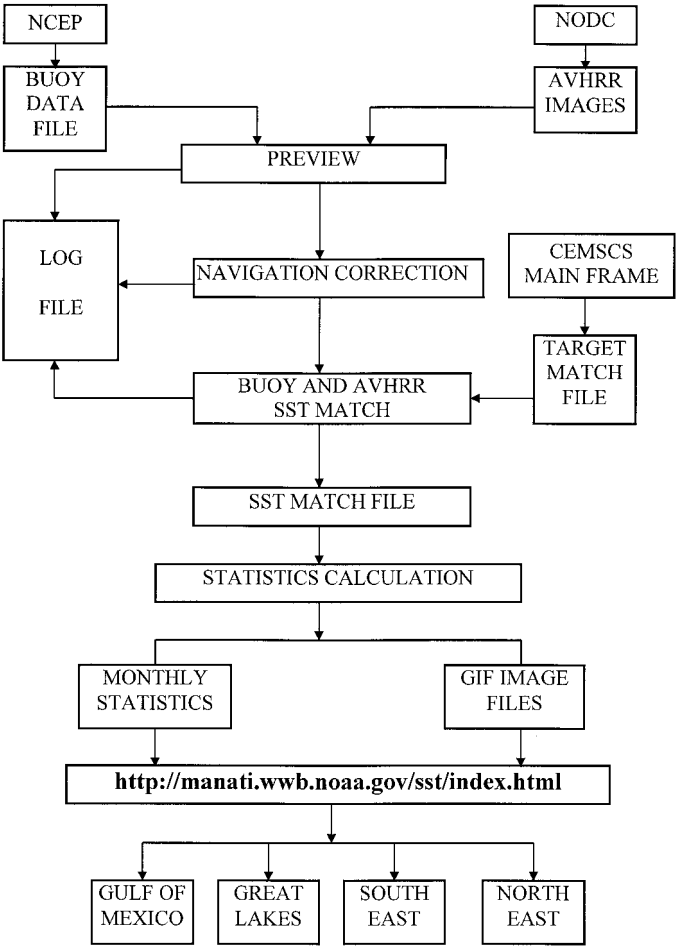

Figure 3. NOAA CoastWatch long-term AVHRR SST validation system.

images (both infrared and visible channels) to see whether an image contains cloud-free SST measurements at any buoy location, (2) overlay coastlines, grids, buoy locations and AVHRR imagery header information on the images, (3) renavigate the imagery by remapping the image to agree with selected ground control points (Krasnopolsky and Breaker 1994), (4) display cloud masks, (5) extract clear 3×3 arrays of CoastWatch SST values centred on each of the buoys in each coastal region, (6) create an output SST match file which contains satellite and buoy SSTs, air temperature, wind and wave information, solar and satellite zenith angles and navigation information, and (7) calculate statistics and make graphic output. Further, cloud screening is done by examining SST and, when necessary, visible imagery. If fog or cloud is suspected, a matchup is not made. Table 3 shows the locations of the NOAA moored buoys used for validation.

4. Validation results

In 1997, the validation was performed in the Gulf of Mexico, Southeast US and Northeast US coastal regions as well as in the Great Lakes region every other month. Both NOAA-12 and NOAA-14 satellite images were validated. The centre value of the 3×3 arrays of SST measurements in the SST match file was taken as the satellite SST. The mean and standard deviation of all the differences in each region were then calculated and stored in the SST match file. During 1997, there were a total of 1829 matchups in the three coastal regions, and 693 matchups in the Great Lakes. The Great Lakes matchups were usually not available in the winter

Table 3. NOAA moored buoys used in the AVHRR SST validation. There are a total of 24 buoys.

Buoy ID	Region	Long.	Lat.
42001	Gulf of Mexico	− 88.6533	25.9283
42002	Gulf of Mexico	− 93.5675	25.8917
42003	Gulf of Mexico	− 85.9142	25.9361
42007	Gulf of Mexico	− 88.7700	30.0900
42019	Gulf of Mexico	− 94.9994	27.8967
42020	Gulf of Mexico	− 96.5056	27.0122
41002	South East	− 75.2406	32.2950
41004	South East	− 79.0994	32.5100
41009	South East	− 80.1842	28.5003
41010	South East	− 78.5019	28.8986
41001	North East	− 72.5897	34.6983
44004	North East	− 70.6897	38.4564
44005	North East	− 68.9439	42.8983
44011	North East	− 66.5833	41.0833
41014	North East	− 74.8336	36.5831
44025	North East	− 73.1667	40.2503
45001	Great Lakes	− 87.7664	48.0481
45002	Great Lakes	− 86.4183	45.3006
45003	Great Lakes	− 82.7681	45.3181
45004	Great Lakes	− 86.5342	47.5458
45005	Great Lakes	− 82.3983	41.6767
45006	Great Lakes	− 89.8667	47.3194
45007	Great Lakes	− 87.0333	42.6833
45008	Great Lakes	− 82.4158	44.2833

when buoy maintenance was performed. In this study, the Great Lakes matchup dataset consists of data from May, July and September 1997.

Due to a calibration error which occurred in NOAA-12 night-time passes from early May to early July of 1997, large SST measurement biases were found for NOAA-12 night-time SSTs. The NOAA-12 night-time SST matchup dataset over this period of time was eliminated. There were a total of 124 and 80 bad data points for the three coastal regions and the Great Lakes region, respectively. That reduced our matchup dataset to 1705 and 613 matchup points.

If the centre value of the 3×3 AVHRR SST array was two standard deviations above or below the nine points mean value, this matchup was not used in the statistics calculation. A significant difference between the centre and the mean value can occur when there is a thermal front in the 3×3 array or some of the 3×3 array points are cloud contaminated. After we excluded the matchups beyond two standard deviations, the remaining matchup totals were 1602 for coastal regions and 572 for the Great Lakes region, respectively. This means that we included about 94% of the matchups from the correctly calibrated dataset in our later analysis.

The number of matches, satellite–buoy bias, and standard deviation of the difference for all coastal regions (Gulf of Mexico, Southeast US and Northeast US) and the Great Lakes region are given in table 4. In addition, the linear correlation coefficients (R) between satellite and buoy measurements are given in table 4. The scatter plots of satellite vs buoy measurements for NOAA-12 and NOAA-14 in the Gulf of Mexico, Northeast US, Southeast US and Great Lakes regions are presented in figures 4(*a*) and (*b*).

5. Discussion

For the three US coastal regions, NOAA-14 AVHRR SSTs calculated with the NLSST algorithm had a bias and standard deviation of 0.16°C and 1.03°C for daytime, and 0.07°C and 0.84°C for night-time. For NOAA-12 daytime SST, the NLSST yields SSTs with a bias of 0.43°C and a standard deviation of 1.00°C. The

Table 4. Mean satellite–buoy SST difference (bias) and standard deviation for NOAA-12 and NOAA-14 satellites in 1997. All 24 moored buoys matched within one pixel (1.1 km at nadir) and an hour of cloud-free satellite data were used in the validation. For the Great Lakes region, the MCSST algorithm is used for daytime SST retrievals; all other measurements are made with the NLSST algorithm. R is the correlation coefficient between AVHRR-derived SST data and buoy measured SST data.

Satellite	Time	Algorithm	Number of matches	(Satellite–buoy) SST bias (°C)	SD (°C)	R
CoastWatch Northeast, Southeast and Gulf of Mexico regions						
NOAA-14	day	NLSST	441	0.16	1.03	0.9911
NOAA-14	night	NLSST	502	0.07	0.84	0.9938
NOAA-12	day	NLSST	374	0.43	1.00	0.9909
NOAA-12	night	NLSST	285	0.20	1.07	0.9896
CoastWatch Great Lakes region						
NOAA-14	day	MCSST	215	0.38	1.01	0.9958
NOAA-14	night	NLSST	157	0.41	0.80	0.9861
NOAA-12	day	MCSST	122	0.26	0.83	0.9930
NOAA-12	night	NLSST	78	1.52	1.27	0.9942

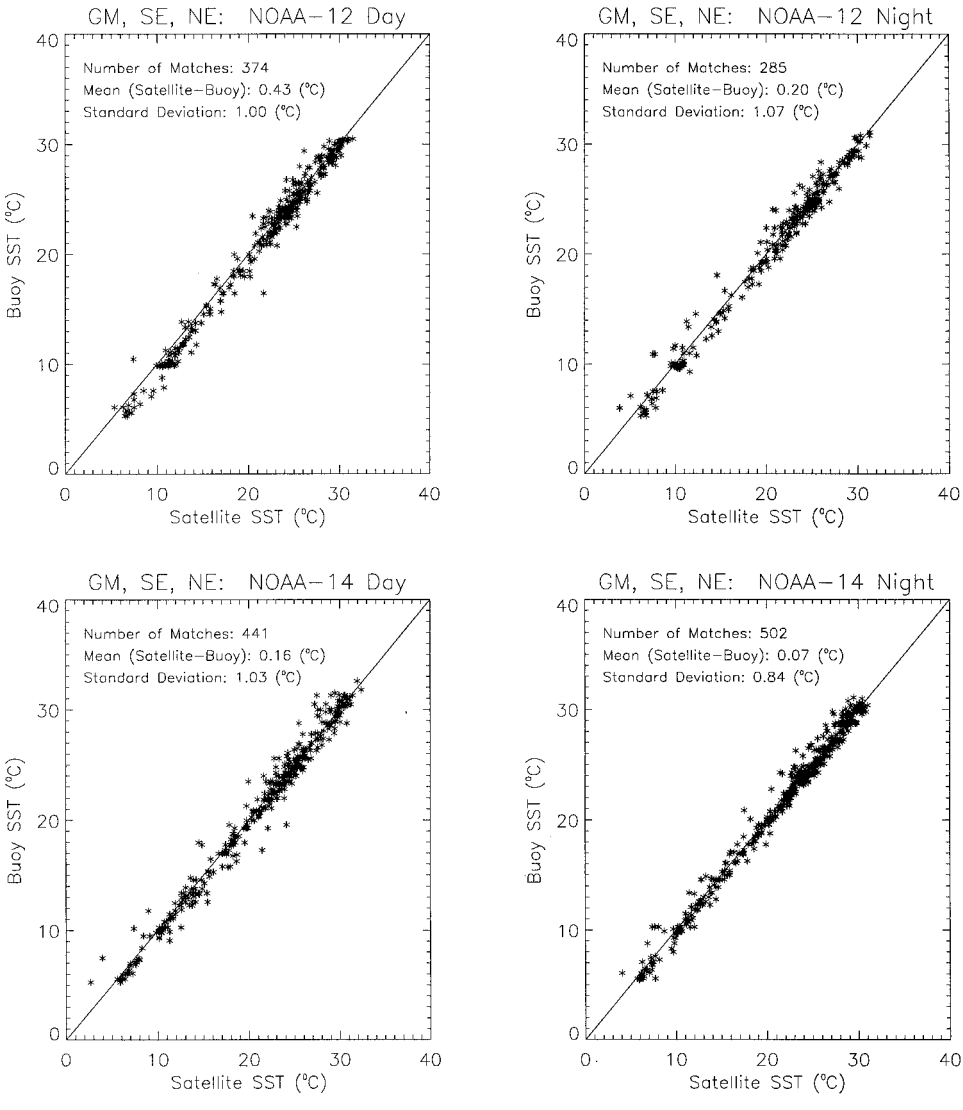

(*a*)

Figure 4. (*a*) Scatter plots of satellite vs buoy measurements for NOAA-12 and NOAA-14 in the Gulf of Mexico (GM), Northeast US (NE) and Southeast US (SE) coastal region for 1997.

bias and standard deviation were 0.20°C and 1.07°C for the NOAA-12 night-time SSTs (table 4).

For the Great Lakes validation, the NLSST-derived NOAA-14 SST measurements had a bias of about 0.4°C for both the day and night algorithms, somewhat higher than the coastal SST estimates. For NOAA-12, the MCSST algorithm gave good SST measurements for daytime SST. However, the NOAA-12 night algorithm had a SST bias as large as 1.52°C. The NOAA-12 satellite local overpass time is around 6:00 to 7:00 am, and our matchup dataset in this region was in the summer

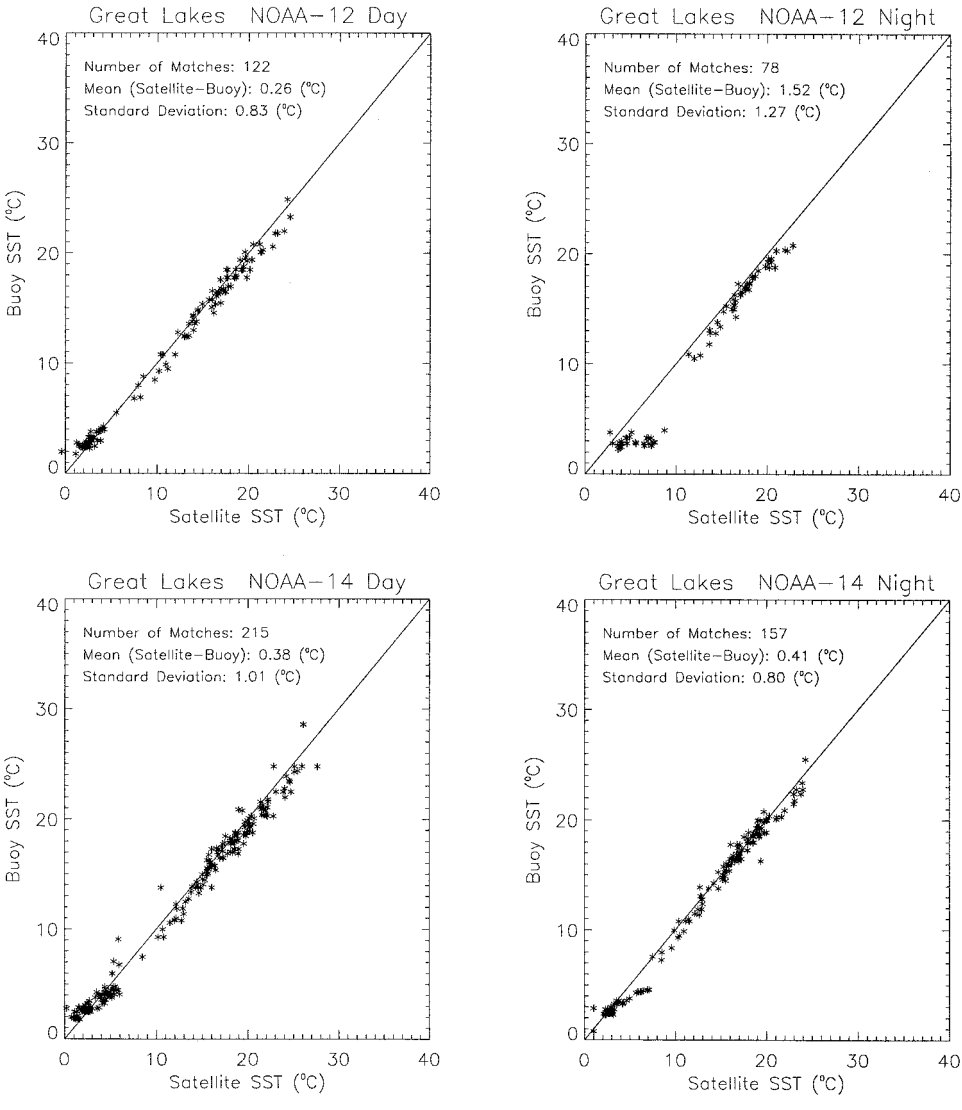

(*b*)

Figure 4. (*b*) Scatter plots of satellite vs buoy SST measurements for NOAA-12 and NOAA-14 in the Great Lakes region.

months (May, July, September). At this time of the day and this time of the year, there is often uniform low level fog over the lake surface. The fog is so thin and its temperature is so close to (but generally higher than) lake surface temperature, that the cloud test did not detect the presence of fog. Therefore, the NOAA-12 night-time algorithm gave large SST biases in the Great Lakes region. We tested the performance of the MCSST algorithm on the NOAA-12 night-time matchup data. The MCSST derived bias is 0.64°C with standard deviation of 2.0°C. Even though, the MCSST algorithm improved the bias from 1.52°C to 0.64°C, the standard deviation is higher. From the scatter plots for NOAA-12 night matchups in figure 4(*b*),

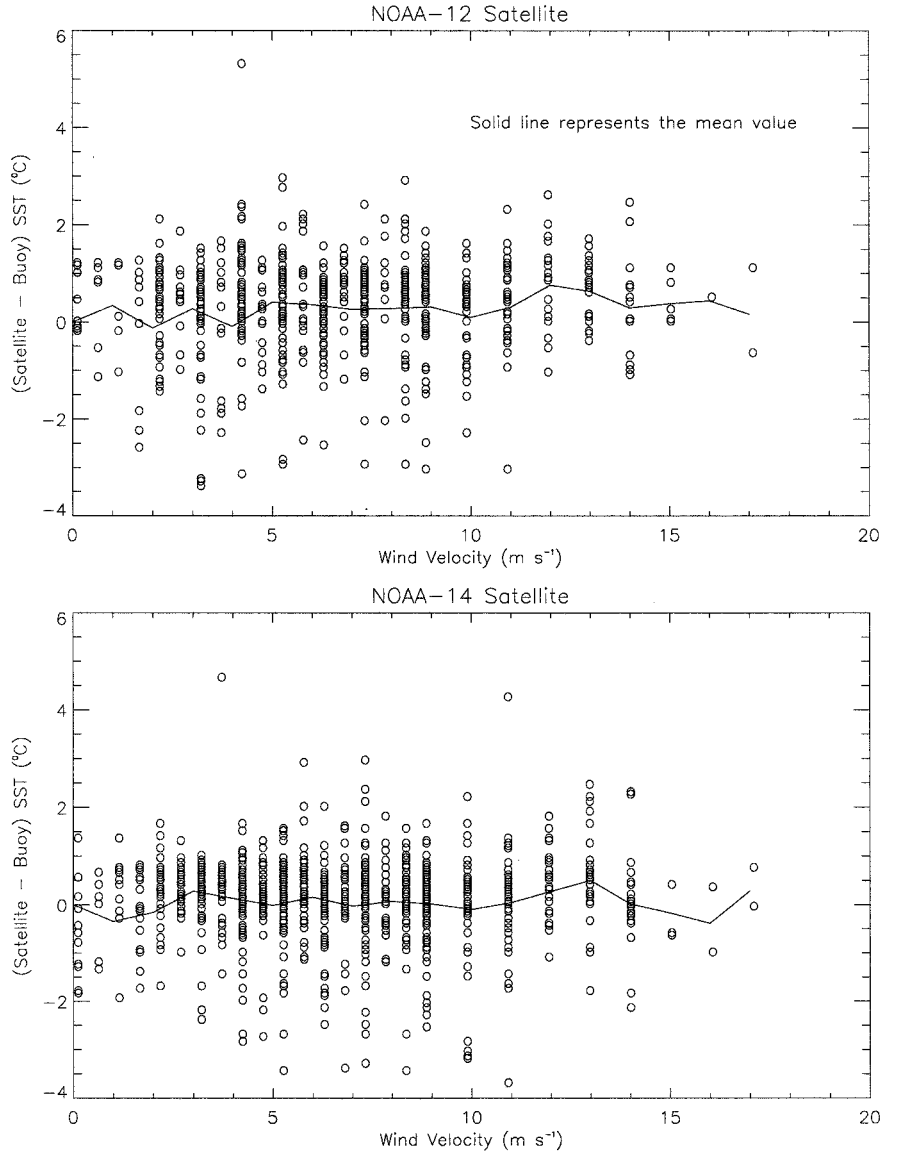

Figure 5. Scatter plots (satellite minus buoy SST measurements) vs wind velocity for the Gulf of Mexico, Northeast US and Southeast US coastal regions for 1997.

we can see there are two schools of matchups. One is at the low temperature end (around 4°C). The other is between 10 and 22°C. From the same figure, we can also see that most of the problems happen when the water temperature is lower than or close to 4°C (this observation is valid for both NLSST and MCSST). After we restrict the satellite and buoy matchups to those above 4°C, the bias and standard deviation for NLSST are 1.01 and 0.60°C; and for MCSST are 0.48 and 1.16°C. The matchups below 4°C come from colder regions of the Great Lakes, and are more susceptible to error caused by warm low clouds (fog) in the early morning during summer.

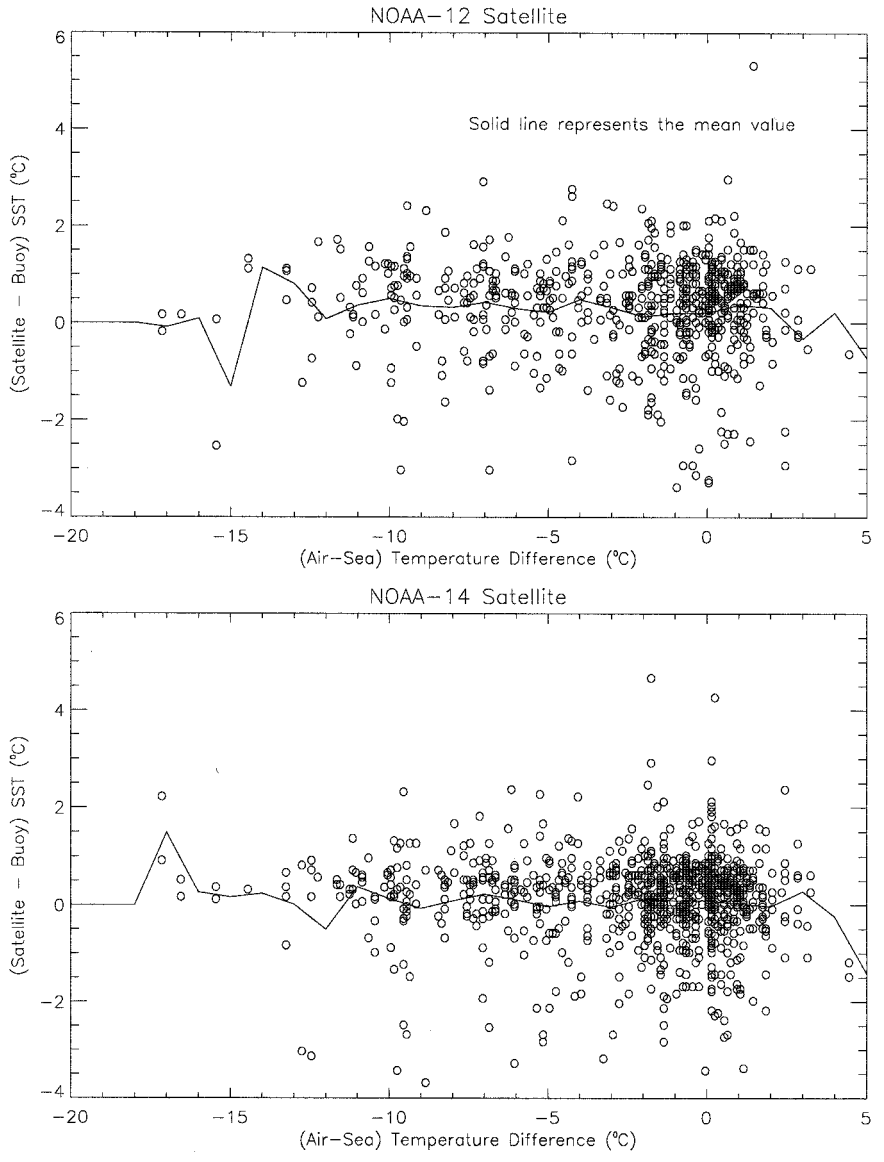

Figure 6. Scatter plots (satellite minus buoy SST measurements) vs air–sea temperature difference for the Gulf of Mexico, Northeast US and Southeast US coastal regions for 1997.

We also plotted the bias of satellite minus buoy SST vs the wind velocity, air–sea temperature difference, satellite zenith angle and channel 4 and 5 brightness temperature difference for the Gulf of Mexico, Northeast US and Southeast US regions in figures 5–8. We did not plot the similar figures for the Great Lakes region because the matchups for Great Lakes region are limited only to the summer. From figure 5 we can see that our SST matchup dataset covered the wind velocity range from 0 to 17 m s^{-1}. The SST bias was about the same in low wind situations as in high wind situations. There was no trend over the air–sea temperature range (figure 6)

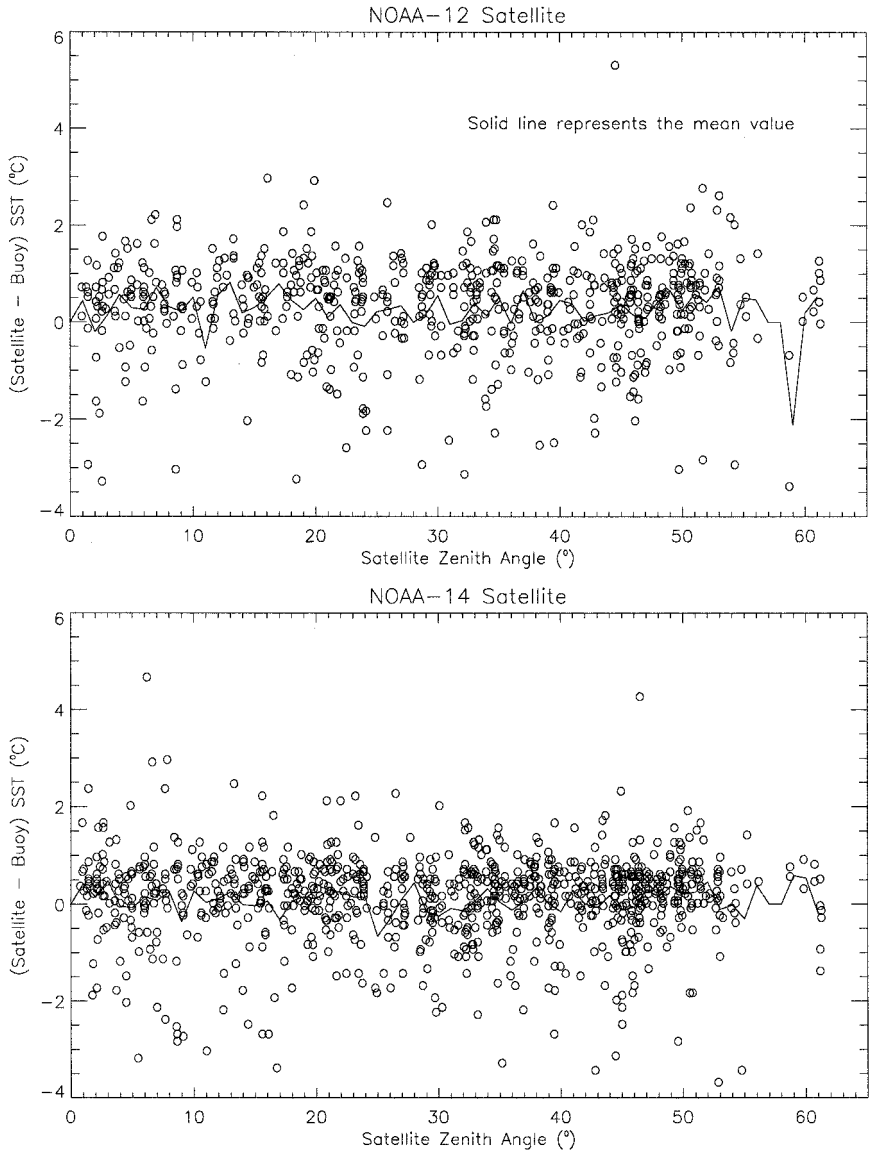

Figure 7. Scatter plots (satellite minus buoy SST measurements) vs satellite zenith angle for the Gulf of Mexico, Northeast US and Southeast US coastal regions for 1997.

from -16°C to about $+5$°C. Also, as the satellite zenith angle varied from 0 to about 62°, the SST bias did not change appreciably. These figures show that, for this set of parameters there was no single dominant factor that contributed to the SST bias. In the development of the NLSST algorithm (Walton *et al.* 1998), it can be seen that the channel 4 and 5 temperature difference is correlated to the atmospheric absorption of infrared radiation. From figure 8 we can see that the NLSST gives good SST measurements over the entire range of channel 4 and 5 temperature difference. This demonstrates the universality of the NLSST algorithm over the range of possible atmospheric water vapour amounts.

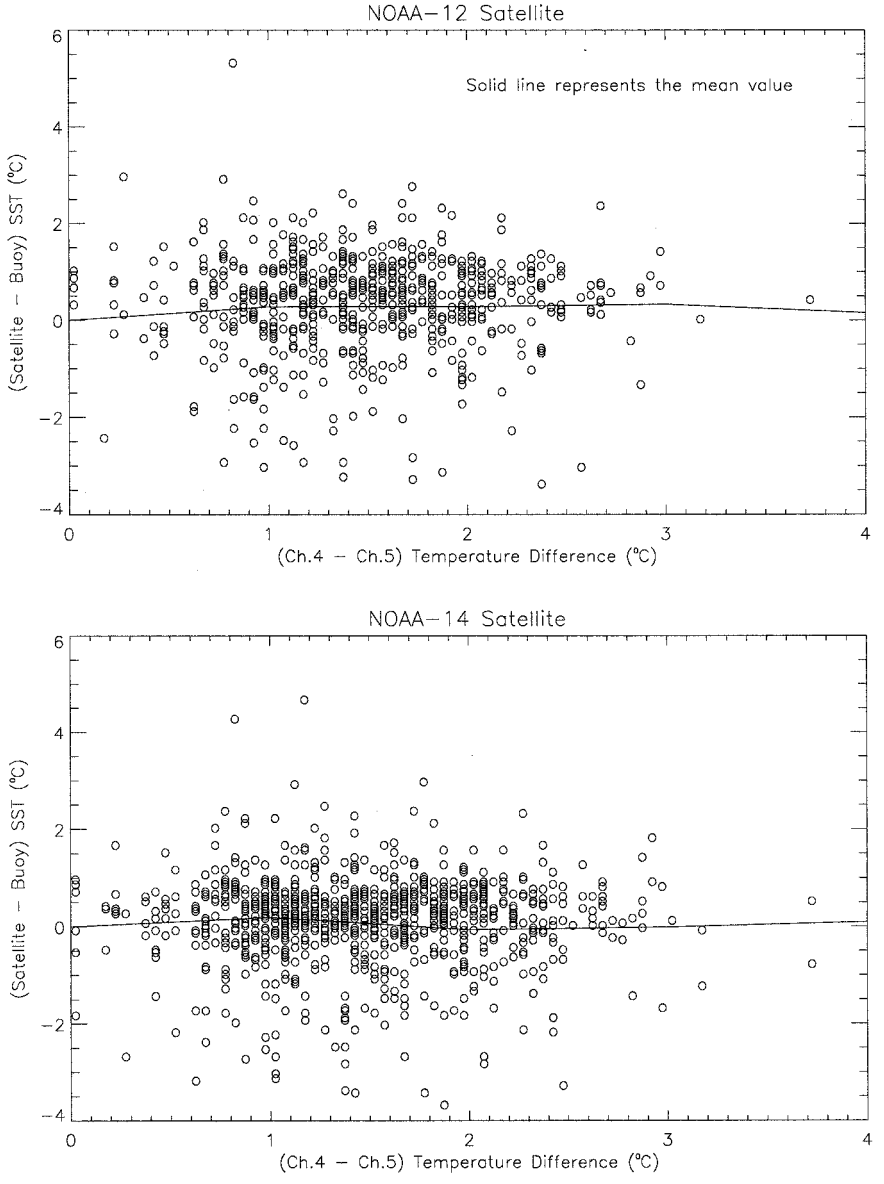

Figure 8. Scatter plots (satellite minus buoy SST measurements) vs AVHRR channel 4 and 5 brightness temperature difference for the Gulf of Mexico, Northeast US and Southeast US coastal regions for 1997.

6. Conclusion

The NOAA/NESDIS operational NLSST SST retrieval algorithm was validated using a matchup dataset of NOAA moored buoys and NOAA-12 and NOAA-14 satellite measurements in three US coastal regions and the Great Lakes in 1997. For the three US coastal regions, both NOAA-14 daytime and night-time SST measurements had a bias less than 0.2°C with a standard deviation about 1°C. For NOAA-12, satellite measurements were also in good agreement with buoy measurements. The bias was between 0.2 and 0.4°C, and the standard deviation was also about 1°C.

For the Great Lakes region, we used the NLSST equation at night and MCSST equation during the day to calculate NOAA-14 SST. The bias for both was about 0.4°C, which was a little bit higher than that of the coastal areas. For NOAA-12, the linear MCSST algorithm gave good results for daytime SST with a bias of about 0.26°C. Due to early morning fog in the summer in the Great Lakes region, the NOAA-12 night-time algorithm yielded a fairly large SST bias.

The NLSST algorithm works well in all the study regions as well as under different wind velocities, air–sea temperature differences, satellite zenith angles and AVHRR channel 4 and 5 temperature differences. Techniques for identifying early morning fog during the summer are required in order to improve night-time SST measurements for the Great Lakes. Simply substituting the MCSST equation for the NLSST equations improves the bias, but increases the standard deviation of satellite–buoy difference.

Acknowledgments

This research was funded by the NOAA/NESDIS Ocean Remote Sensing Program and the NOAA CoastWatch Program.

References

Anding, D., and Kauth, R., 1970, Estimation of sea-surface temperature from space. *Remote Sensing of Environment*, **1**, 217–220.

Barton, I., 1983, Dual channel satellite measurements of sea surface temperature. *Quarterly Journal of the Royal Meteorological Society*, **109**, 265–378.

Barton, I., Zavody, A., O'Brien, D., Cutten, D., Saunders, R., and Llewellyn-Jones, D., 1989, Theoretical algorithms for satellite-derived sea surface temperatures. *Journal of Geophysical Research*, **94**, 3365–3375.

Barton, I., 1995, Satellite-derived sea surface temperature: current status. *Journal of Geophysical Research*, **100**, 8777–8790.

Böhm, E., Marullo, S., and Santoleri, R., 1991, AVHRR visible–IR detection of diurnal warming events in the western Mediterranean Sea. *International Journal of Remote Sensing*, **12**, 695–701.

Breaker, L., Krasnopolsky, V., Rao, D. B., and Yan, X. H., 1994, The feasibility of estimating ocean surface currents on an operational basis using satellite feature tracking methods. *Bulletin of the American Meteorological Society*, **75**, 2085–2095.

Cayula, J. F., and Cornillon, P., 1992, Edge detection algorithm for SST images. *Journal of Atmospheric and Oceanic Technology*, **9**, 67–80.

Cornillion, P., and Stramma, L., 1985, The distribution of diurnal sea surface warming event in the western Sargasso Sea. *Journal of Geophysical Research*, **90**, 11811–11815.

Cornillion, P., 1989, Sea surface temperature products for the Oceanography Scientific Research Community. A report of the Sea Surface Temperature Archiving Science Working Group, sponsored by NASA and NOAA, Joint Oceanographic Institutions, Inc., Washington, DC, 36 pp.

Emery, W. J., and Fowler, C. W., 1991, Fram Strait satellite image-derived ice motion. *Journal of Geophysical Research*, **96**, 4751–4768.

Emery, W. J., Yu, Y., Wick, G. A., Schluessel, P., and Reynolds, R. W., 1994, Correcting infrared satellite estimates of sea surface temperature for atmospheric water vapor attenuation. *Journal of Geophysical Research*, **99**, 5219–5236.

Harries, J. E., Llewellyn-Jones, D. T., Minnett, P. J., Saunders, R. W., and Zavody, A. M., 1983, Observation of sea-surface temperature for climate research. *Philosophical Transactions of the Royal Society of London Series A*, **309**, 381–395.

Hawkins, J. D., Clancy, R. M., and Price, J. F., 1993, Use of AVHRR data to verify a system for forecasting diurnal sea surface temperature variability. *International Journal of Remote Sensing*, **12**, 1347–1357.

Kahru, M., Håkansson B., and Rud, O., 1995, Distributions of the sea-surface fronts in the Baltic Sea as derived from satellite imagery. *Continental Shelf Research*, **15**, 663–679.

Krasnopolsky, V. M., and Breaker, L. C., 1994, The problem of AVHRR image navigation revisited. *International Journal of Remote Sensing*, **15**, 979–1008.

Llewellyn-Jones, D. T., Minnett, P. J., Saunders, R. W., and Zavody, A. M., 1984, Satellite multichannel infrared measurements of sea surface temperature of the N. E. Atlantic Ocean using AVHRR/2. *Quarterly Journal of the Royal Meteorological Society*, **110**, 613–631.

May, D. A., and Holyer, R. J., 1993, Sensitivity of satellite multichannel sea surface temperature retrievals to the air–sea temperature difference. *Journal of Geophysical Research*, **98**, 12567–12577.

McClain, E. P., Pichel, W. G., and Walton, C. C., 1985, Comparative performance of AVHRR-based multi-channel sea surface temperatures. *Journal of Geophysical Research*, **90**, 11587–11601.

Mcmillin, L. M., 1975, Estimation of sea surface temperature from two infrared window measurements with different absorption. *Journal of Geophysical Research*, **80**, 5113–5117.

Mcmillin, L. M., and Crosby, D. S., 1984, Theory and validation of the multi window sea surface temperature from space. *Journal of Geophysical Research*, **89**, 3655–3661.

Minnett, P., 1990, The region optimization of infrared measurements of sea surface temperature from space. *Journal of Geophysical Research*, **95**, 13497–13510.

Pearce, A. F., Prata, A. J., and Manning, C. R., 1989, Comparison of NOAA/AVHRR-2 sea surface temperature with surface measurement in coastal waters. *International Journal of Remote Sensing*, **10**, 37–52.

Pichel, W. G., 1991, Operational production of multichannel sea surface temperatures from NOAA polar satellite AVHRR data. *Palaeogeography, Palaeoclimatology, Palaeoecology*, **90**, 173–177.

Planet, W. G., 1998, Data extraction and calibration of TIROS-N/NOAA radiometers. NOAA Technical Memorandum NESS 107, Rev. 1, US Department of Commerce, NOAA/NESDIS, Washington, DC, 105.

Robinson, I. S., and Ward, N., 1989, Comparison between satellite and ship measurements of sea surface temperature in the north-east Atlantic ocean. *International Journal of Remote Sensing*, **10**, 787–799.

Shenoi, S. C., 1999, On the suitability of algorithms for the retrieval of SST from the north Indian Ocean using NOAA/AVHRR data. *International Journal of Remote Sensing*, **20**, 11–29.

Stowe, L. L., McClain, E. P., Carey, R., Pellegrino, P., Gutman, G. G., Davis, P., Long, C., and Hart, S., 1991, Global distribution of cloud cover derived from NOAA/AVHRR operational satellite data. *Advanced Space Research*, **11**, 51–54.

Strong, A. E., and McClain, E. P., 1984, Improved ocean surface temperatures from space-comparisons with drifting buoys. *Bulletin of the American Meteorological Society*, **65**, 138–142.

Topliss, B. J., 1995, A review of satellite sea surface temperature validations for NOAA's 7, 9 and 11 using imagery off eastern Canada. *Canadian Journal of Remote Sensing*, **21**, 492–510.

Walton, C. C., 1988, Nonlinear multichannel algorithms for estimating sea surface temperature with AVHRR satellite data. *Journal of Applied Meteorology*, **27**, 115–124.

Walton, C. C., Pichel, W. G., Sapper, J. F., and May, D. A., 1998, The development and operational application of non-linear algorithms for the measurement of sea surface temperatures with the NOAA polar-orbiting environmental satellites. *Journal of Geophysical Research*, **103**, 27 999–28 012.

Yates, H., Cotter, D., and Ohring, G., 1985, ENVIROSAT-2000 Report, Operational Satellite Support to Scientific Programs, NOAA, Washington DC, 50.

Yokoyama, R., and Tanba, S., 1991, Estimation of sea surface temperature via AVHRR of NOAA-9—comparison with fixed buoy data. *International Journal of Remote Sensing*, **12**, 2513–2528.

Yokoyama, R., Tanba, S., and Souma, S., 1993, Air–sea interacting effects to the sea surface temperature observation by NOAA/AVHRR. *International Journal of Remote Sensing*, **14**, 2631–2646.